Accepted Manuscript

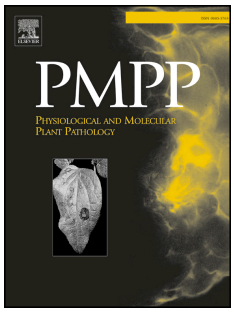

Transcriptional analysis and histochemistry reveal a dominant role for cell wall signaling in mediating *Pythium myriotylum* resistance in *Zingiber zerumbet*

Kiran Ayyanperumal Geetha, Sayuj Koyyappurath, Lesly Augustine, George Thomas

PII: S0885-5765(18)30242-X

DOI: https://doi.org/10.1016/j.pmpp.2018.11.002

Reference: YPMPP 1371

To appear in: *Physiological and Molecular Plant Pathology*

Received Date: 21 August 2018

Revised Date: 10 October 2018

Accepted Date: 14 November 2018

Please cite this article as: Geetha KA, Koyyappurath S, Augustine L, Thomas G, Transcriptional analysis and histochemistry reveal a dominant role for cell wall signaling in mediating *Pythium myriotylum* resistance in *Zingiber zerumbet*, *Physiological and Molecular Plant Pathology* (2018), doi: https://doi.org/10.1016/j.pmpp.2018.11.002.

Transcriptional analysis and histochemistry reveal a dominant role for cell wall signaling in mediating *Pythium myriotylum* resistance in *Zingiber zerumbet*

Kiran Ayyanperumal Geetha[1], Sayuj Koyyappurath[1], Lesly Augustine[2] and George Thomas[1*]

Affiliation:

[1]Plant Disease Biology & Biotechnology, Rajiv Gandhi Centre for Biotechnology, Thiruvananthapuram, Kerala, India

[2]Assistant Professor, Department of Botany, Sacred Heart College, Kochi, Kerala, India

*** Correspondance:**

George Thomas
Plant Disease Biology & Biotechnology
Rajiv Gandhi Centre for Biotechnology
Thiruvananthapuram – 695 014
Kerala, India
E-mail: gthomas@rgcb.res.in

Abstract

Although post infection changes in cell wall constituents are known to induce the immune response in plants against necrotrophs, little is known about the role of the cell wall in mediating resistance in *Zingiber zerumbet* (L.) Smith (Zingiberaceae) against the soil-borne necrotrophic oomycete *Pythium myriotylum* Drechsler, which causes soft-rot disease. Using RNA-Seq in combination with custom gene expression microarray we studied the temporal expression profile of 46 wall-associated genes in *Z. zerumbet* against *P. myriotylum* inoculation. Many genes that promote cell wall loosening were suppressed. Similarly, the genes involved in the biosynthesis and the signaling of phytohormones and the receptor-like kinases that mediate cell elongation were also suppressed. Several monolignol biosynthetic pathway genes were up-regulated. Histochemistry of the collar region of the aerial stem revealed H_2O_2 accumulation, increased lignification of the mesophyll cells surrounding vascular bundles in the leaf sheath and the significant increase in total lignin content. Pathogen hyphae were restricted to peripheral leaf sheath and were not extended into the pith through which the principal portion of the connective tissues passes in the aerial stem. Results highlight a coordinated transcriptional reprogramming of cell wall-associated genes to bring about changes in cell wall composition to minimize the cell wall damage caused by pathogen factors and to render the cell wall less amenable to pathogen penetration. The study illustrates a key role for cell wall fortification in preventing pathogen colonization in the vascular tissues, thus ensuring the transport system remains unaffected by the pathogen invasion.

Running head: *Pythium* resistance in *Z. zerumbet*

Key words: *Zingiber zerumbet*, *Pythium*, soft-rot disease, transcriptome, microarray, lignification.

Introduction

More than 300 species are reported in the soil-borne necrotrophic oomycete genus *Pythium*. Many of the *Pythium* spp. are economically important pathogens and cause root rot and damping off disease in several plant species [1,2]. Almost 15 species of *Pythium* are known to cause soft rot disease in spice crop ginger (*Zingiber officinale* Roscoe, Zingiberaceae) [1]. Soft rot disease is a major constraint to ginger production in all ginger producing countries in the world. In ginger, the *Pythium* infection radiates from the intersection (collar) between the aerial-stem and the rhizome. The pathogen colonizes and rots the rhizome within seven to ten days [1,3].

It is extremely difficult to control *Pythium* pathogens by cultural, chemical or biological measures. Natural resistance against this pathogen is rare in plants [2]. In the previous studies, we identified durable resistance against *Pythium* infection in certain accessions of *Z. zerumbet* (L.) Smith, a wild congener of cultivated ginger [3]. Relatively little is known about the molecular basis of host defense against *Pythium* infection in plants. Previous studies implicate a dominant role for jasmonic acid (JA) signaling in the induction of host immunity against *Pythium* [4,5]. De Vleesschauwer *et al.,* [6] showed that *P. graminicola* hijacks the brassinosteroid (BR) signaling machinery in rice and exploits BRs as virulence factors to inflict disease. *De novo* transcriptome analyses produced high enrichment of transcripts associated with multiple defense pathways in a resistant genotype of *Curcuma longa* in response to *P. aphanidermatum* infection and, based on which, the authors concluded that *C. longa* adopts multiple strategies to defend *P. aphanidermatum* attack [7]. In our previous analyses, although transcriptional reprogramming has occurred for many genes in *Z. zerumbet* in response to *Pythium*, the involvement of any particular gene or pathway in host defense was not discernible from the expression profile [8, 9].

The plant cell wall is the primary barrier to be faced with by an invading pathogen. The signaling emanates from the interaction between the host cell wall, and a necrotrophic pathogen activates multiple signaling cascades in the host. Among them, the most important one is the extensive cell wall remodeling triggered by both host and pathogen enzymes [10]. The necrotrophs induce the production of pectin methylesterase (PME) enzyme in the host [11]. The PME activity demethylesterify the cell wall pectin homogalacturonan (HG). The demethylesterified HG is more readily cleaved by the cell wall degrading enzymes (CDEs) polygalacturonases (PGs) and pectate lyases (PLEs) secreted by the pathogen. The degradation of host cell wall by CDE initiates pathogen colonization process in the host tissues [11,12]. The HG demethylesterification also renders it more susceptible to host's own PMEs and PLEs [13,14]. The suppression of the host *PG* or *PLE* enhances host resistance to pathogens [13,14]. The PME, PLE, and PG together with the xyloglucan endotransglucosylase/hydrolases (XTH) enzyme loosen the cell wall and positively regulate cell elongation in growing tissues [15, 16]. The pathogen easily breaches the loosed cell wall and successfully colonize the elongating tissues [15, 17]. Suppression of cell expansion contributes to pathogen resistance in *PLE* mutants [13]. Another important aspect of the HG degradation by pathogen CDEs is the production of the defense signaling molecule oligogalacturonides (OGs) [11, 12]. The OGs act as damage-associated molecular pattern in the host (DAMP), bind with the receptor wall-associated kinases (WAKs) and activate host immune systems [18]. The hormones brassinosteroids (BR), auxin and gibberellic acid (GA) that promote cell elongation have a key role in regulating host defense against necrotrophs [10, 15, 19].

116 The lignification and the cell wall strengthening is another important strategy
117 employed by the host to suppress necrotroph infection [20]. Monolignols are
118 polymerized into lignin in the apoplast via the oxidative reaction by peroxidases in the
119 presence of H_2O_2 [21]. Therefore, a marked increase in peroxidase activity and H_2O_2
120 accumulation precede cell wall lignification during the resistance reactions of a host
121 against necrotrophic pathogens [20, 22]. In *Arabidopsis*, the inactivation of the genes
122 *CELLULOSE SYNTHASES 4* /*IRREGULAR XYLEM5* (*CESA4*/*IRX5*) and *WALLS*
123 *ARE THIN1* (*WAT1*) that are involved in cellulose deposition in the secondary cell
124 wall confer resistance to necrotrophic pathogens [23, 24]. The disruption of cellulose
125 biosynthesis triggers lignin biosynthesis and pathogen defense [25].
126 The role of cell wall remodeling genes in mediating host response to *Pythium*
127 has not been yet examined in plants. RNA-seq coupled with gene expression
128 microarray or real time quantitative PCR (RT-qPCR) analysis is a method of choice
129 for studying gene expression kinetics in the non-model organism [26]. In this study,
130 we examined the expression kinetics of cell wall-related genes, which constituted one
131 of the most prominent and significantly enriched gene ontology terms in RNA-seq
132 data obtained in *Z. zerumbet* in response to *P. myriotylum*. We also examined the
133 histochemical changes in *Z. zerumbet* during *P. myriotylum* pathogenesis.
134
135 **Materials and Methods**
136 **Plant materials, pathogen inoculation and tissue sampling**
137 The *Z. zerumbet* accession 2010-9, which is immune to soft-rot disease [3] was used
138 for inoculation studies. Rhizomes harvested from mature plants were germinated in
139 earthen pots in autoclaved red-earth: river-sand: leaf compost (1:1:1) and the plants
140 were maintained in an insect-protected net-house under natural conditions at Rajiv

Gandhi Centre for Biotechnology. An aggressive *Pythium myriotylum* Drechsler isolate (RGCB N14), purified from rhizomes collected from soft-rot infected ginger plants sampled from farmer's field in Kerala, was used for inoculation experiments. *P. myriotylum* is the prevalent species causing soft rot disease in ginger in India [27]. The pathogen was identified based on ITS-2 sequence identity as reported previously [28]. Virulence of this pathogen isolate was tested on the ginger variety Varada. The Varada plants were wilted completely within three weeks after inoculation and the speed and pattern of disease progression was identical to that yielded by *Pythium aphanidermatum* (RGCB117) in the previous study [8, 9]. The pathogen was maintained at room temperature (25°C) in potato dextrose agar (PDA) medium with periodic sub-culturing and virulence testing.

The collar region of four months old plants with uniform growth habits was inoculated with four 10 mm diameter mycelial discs excised from the growing margins of a 48 h old *P. myriotylum* culture grown on PDA. The inoculated region was covered with wet cotton to provide sustained humidity. Plants mock inoculated with plain PDA discs were used as controls. Similar to the response to *P. aphanidermatum* (RGCB117) [3], the *Z. zerumbet* accession 2010-9 was immune to *P. myriotylum* (RGCBN4) also. For RNA isolations, one-inch long collar tissue was collected, flash chilled in liquid nitrogen and stored at -80°C until further use.

De novo assembly and annotation

We developed two RNA-seq libraries in *Z. zerumbet*: one from RNA samples isolated from untreated control and the other using RNA sample isolated from plants 24 hours post inoculation (hpi) with *P. myriotylum* (NCBI Sequence Read Archive accession numbers: control - SRA SRX959143; treated - SRX 959144). Total RNA was isolated

by the method of [29]. As our interest in deep sequencing was to generate a pool of differentially expressed transcripts to develop a gene expression microarray, we limited the sequencing to a single replicate for control and treated samples. Transcriptome libraries were constructed with an IlluminaTruSeq RNA library Prep kit (Illumina, San Diego, California, USA). The libraries were sequenced using an Illumina GAIIx platform employing paired-end module with 73/72 base read length. The sequencing was carried out at Genotypic Technology PVT. LTD, Bengaluru, India. Quality of the raw reads was tested using the software NGS QC Toolkit (Version 2.2.3). The reads containing adaptor sequences and unknown nucleotides were removed and reads with ≥ 70% bases with ≥ 20 Phred score were filtered as high quality reads. High quality reads obtained from control and treated samples were pooled and were subjected to *de novo* assembly using a de Bruijn graph method as implemented in Trinity assembler-Version 20140717 using default parameters. The quality of the Trinity assembled contigs was tested based on the number of reads aligned onto contigs (number of reads ≥ 10) and the FPKM (fragments per kilobase of exon per million fragments mapped) values (value ≥ 1) and the truly assembled contigs were filtered out. In the next step, distinct transcripts were derived by clustering truly assembled contigs at a 90% identity threshold using the software CD-HIT-EST (Version 4.6.1) and filtered the longest contigs (transcript) from each assembled Trinity locus.

The distinct transcripts were annotated by performing homology searches against NCBI, non-redundant (nr) Viridiplantae database using BLASTx tool (http://blast.ncbi.nlm.nih.gov/Blast.cgi) with an E-value cut-off ≤ 10^{-5}. Transcripts showing homology to pathogens (oomycetes or stramenopile) and to the organisms other than the ones listed in the Viridiplantae database were not included in further

191 analysis. The distinct and annotated plant-specific transcripts were designed as
192 'unitranscripts'.
193
194 **Digital gene expression and gene ontology enrichment**
195 High quality reads obtained in control and treated samples were aligned separately
196 against each unitranscript using the software Bowtie (Version 2.2.4) and the number
197 of reads mapped from the two libraries was extracted using the Samtools idxstats
198 command. The fold difference between the number of reads that mapped onto each
199 unitranscript from the transcriptome libraries generated from control and treated
200 samples was estimated (digital gene expression, DGE) using the software package
201 DESeq2. Unitranscripts with a fold change $\geq {}^{+}2.0$ and $\leq {}^{-}2.0$ between treated and
202 control samples were considered significantly up-regulated and down-regulated
203 respectively.
204 Gene ontology (GO) enrichment analysis was performed on unitranscripts
205 using the software AgriGO and identified significantly ($p < 0.05$) enriched gene
206 ontologies in the dataset using Fischer's exact test.
207
208 **Microarray and RT-qPCR validation of unitranscripts**
209 The custom gene expression microarray analysis was performed at the University of
210 Delhi South Campus Microarray Centre (UDSCMAC), University of Delhi, India.
211 Briefly, the probes were designed against *de novo* assembled transcripts using the
212 program eArray (Agilent Technologies, Santa Clara, CA, USA;
213 https://earray.chem.agilent.com/erray/). The designed oligonucleotide probes were
214 printed onto 1 x 3 inch glass slides using the SurePrint Ink-jet technology (Agilent
215 Technologies) in an 8 x 60k format. The RNA samples isolated from two biological

replicates each from *Z. zerumbet* at 0hpi (untreated control) and at 18hpi, 36hpi and 48hpi were used for array hybridizations. The RNA isolated from tissues sampled from an independent plant constituted a biological replicate. The hybridization procedure was performed according to the Agilent Technologies' 'One-colour Microarray-based Gene expression analysis protocol' (G4140-90040) using the Gene Expression Hybridization Kit (5188-5279). The hybridization was performed in a hybridization oven (G2505-80085, Agilent Technologies) and washed slides were scanned using a scanner (G2565CA, Agilent Technologies). The data analysis was performed by using the software Genespring GX12 (Agilent Technologies). The significance ($p < 0.05$) in the quantity of transcripts (fold change) from treated samples (18hpi, 36hpi, 48hpi) hybridized to a probe in relation to the untreated control (0hpi) were determined by Student's *t*-test. Heat maps were constructed using the fold change values with the online program ClustVis.

RT-qPCR primers were designed based on the transcriptome data developed in the present study. Primers were designed using the software Primer Express (Version 3.0, Applied Biosystems, Foster City, CA, USA) and were custom synthesised with Sigma (Sigma Genosys, Bengaluru, India). RT-qPCR was performed on a CFX96 real-time system (Bio-Rad, Hercules, CA, USA) using iQ™*SYBR*® Green Supermix (Bio-Rad). RNA samples isolated from *Z. zerumbet* at 0hpi (control) 12hpi, 24hpi, 36hpi, 48hpi and 60hpi with *Pythium* were included in RT-qPCR. cDNA was synthesised from DNase I treated total RNA samples using BluePrint RT reagent kit (Takara Bio Inc. Japan) following the manufacturer's instructions. Three independent biological replicates were used at each time points with two technical replicates for each biological replicate. Cq values from Bio-Rad CFX manager (Version 1.6, Bio-

Rad) were exported to the software qbasePLUS (Biogazelle, Belgium) and fold change in transcript abundance was estimated for each gene in the treated sample in $\log_2$ scale in relation to control after normalizing with reference genes *Actin1* and *eEF1*. Statistical significance of $\log_2$ transformed fold changes was tested by t-test ($p < 0.05$).

Selection of gene set

The genes that belong to the selected significantly enriched GO classes identified in the *Z. zerumbet* transcriptome library were retrieved from NCBI, non-redundant (nr) Viridiplantae database and developed local databases. The unitranscripts were blasted against the local database and filtered the homologues with an E-value cut off $\leq 10^{-4}$ and 65% identity score. The filtered unitranscripts that showed significant differential expression in DGE analysis and in at least one of the time periods in microarray or RT-qPCR analyses, and whose orthologous have known defence-related functions in other plant species were included in the study.

Histochemical methods

To examine the aerial-stem anatomy, transverse hand sections (approx. 90 - 100 µm) of the collar region from the uninoculated control plants were stained with Safranin-O (in 50% EtOH). For histochemical staining and lignin quantification collar region of the aerial-stem were sampled from three individual plants each from uninoculated controls and at 12hpi, 24hpi and 48hpi with *P. myriotylum*. The pattern of pathogen ingress in host tissue was determined by the lactophenol-trypan blue staining of longitudinal hand sections. Phloroglucinol-HCl staining of the transverse hand sections was performed to visualize the lignin in host cell walls. The H_2O_2

accumulation in the host tissue following pathogen inoculation was examined by 3, 3′-diaminobenzidine (DAB) staining of longitudinal hand sections. In all cases, the stained sections were viewed and photographed at 40 X magnification under bright-field illumination on a Nikon Eclipse Ni-E (Nikon, Tokyo, Japan) microscope. The total cell wall bound soluble lignin was quantified in the host tissue by using the acetyl bromide method [30].

Results

RNA-seq analysis and the selection of gene set

The NGS QC Toolkit treatment filtered 32.9 million and 31.8 million high quality reads from control and treated samples of *Z. zerumbet*, respectively. More than 90% of the reads obtained in the libraries were of high quality with an average of 98% of bases showing a Phred score > 20. The *de novo* assembly of raw reads and the downstream analyses of the synthesized transcripts as described in Materials and Methods produced 23620 annotated unitranscripts in *Z. zerumbet*. GO terms involved in cell wall-related functions including phenylpropanoid metabolism and cell wall organization were predominant among the significantly enriched biological process GO classes identified in the transcriptome database. Previously, the transcriptome profiling of post inoculated *Z. zerumbet* hardly produced any wall related genes in a limited pool of 20 differentially modulated genes yielded by mRNA differential display analysis [8]. Cell wall signalling and remodelling have a key role in orchestrating host defense against necrotrophic pathogens [10]. In this study, we focused on the functional bearing of the expression kinetics of cell wall-associated genes in the incompatible reactions of *Z. zerumbet* against *P. myriotylum*.

The genes involved in cell wall associated functions including biosynthesis and signalling of BR, GA and auxin were retrieved from NCBI, non-redundant (nr) Viridiplantae database and developed local databases. The unitranscripts sequences were blasted against the local database and the unitranscripts that are homologous to wall-associated genes from other plant species (orthologous genes) were filtered at an E-value cut off $\leq 10^{-4}$ and 65% identity score. The unitranscripts with significant DGE value were further sorted out from the filtered unitranscripts and examined the temporal expression profiles produced by these unitranscripts in microarray analysis. Finally, transcripts of a set of 46 wall-associated genes with known defense-related functions in other plant species and whose transcripts showed significant modulation in DGE analysis and in at least one of the time periods in microarray analysis in *Z. zerumbet* following *P. myriotylum* treatment were chosen (Table S1). Temporal expression pattern of a randomly selected set of four unitranscripts was validated by RT-qPCR (Table S1). The selected gene set consisted of genes involved in cell wall remodeling, monolignol biosynthesis and lipid polymerization and biosynthesis and signaling of phytohormones BR, GA and auxin.

Cell wall remodeling

The quantity of the transcripts of the *PME*, *PG* and *PLE* genes were significantly declined in *Z. zerumbet* following *P. myriotylum* inoculation (Fig. 1; Table S1). A gene encoding a BURP domain-containing protein 12 (*BURP12)* with a role in pectin cleavage and cell expansion [31] was strongly down-regulated. However, the gene *QUARTET3* (*QRT3*) which encode a protein with polygalacturonase activity [32] was triggered in *Z. zerumbet* at 36 hpi. Similarly, *PLASMA MEMBRANE H+ATPase* (*PM H+ATPase)*, which regulates the apoplastic pH [33] was strongly induced following pathogen inoculation. Transcripts of two members of the *WAK* gene family (*WAK2*-

315 *LIKE)* were significantly accumulated in *Z. zerumbet*, especially at the early period of
316 infection (Fig. 1; Table S1).

317 Transcripts of three members of the *XTH* gene family, *XTH8*, *XTH30* and
318 *XTH33* were reduced following pathogen inoculation in *Z. zerumbet*. Three receptor-
319 like kinase genes *FERONIA* (*FER*), *ERECTA* (*ER*) and *HERCULES 1* (*HERK1*) that
320 have a key role in cell expansion, were also down-regulated [34, 35] (Fig. 1; Table
321 S1).

322 The plasma membrane-localized *CESA4*/*IRX5* gene, which is required for
323 cellulose deposition in the secondary cell wall [23] was strongly down-regulated in *Z.*
324 *zerumbet* following *P. myriotylum* inoculation. Similarly, transcripts of *WAT1*,
325 another gene involved in secondary cell wall deposition and cell-elongation [24] was
326 also declined following pathogen inoculation in *Z. zerumbet*. The analysis identified
327 the strong induction of *INV3*, a member of sucrose cleaving cell wall invertase gene
328 family [36]. Two genes belonging to the membrane-localized sugar transport gene
329 family Sugars Will Eventually be Exported Transporters (*SWEET*) [37] were
330 negatively altered in *Z. zerumbet* following *P. myriotylum* inoculation (Fig. 1; Table
331 S1).

332 **Monolignol biosynthesis and lignin polymerization**

333 *PHENYLALANINE AMMONIA-LYASE* (*PAL*), the core gene involved in the
334 phenylpropanoid biosynthetic pathway [21] was induced in *Z. zerumbet* following
335 pathogen inoculation (Fig. 2; Table S1). Transcripts of the genes involved in the
336 monolignol biosynthetic pathway including *4-COUMARATE-CoA LIGASE 2* (*4CL2*),
337 *CINNAMOYL*-CoA *REDUCTASE* (*CCR*), *CAFFEIC ACID*/*5-HYDROXYFERULIC*
338 *ACID O-METHYLTRANSFERASE 1* (*COMT1*) and *CINNAMYL ALCOHOL*

DEHYDROGENASE 2 (*CAD2*) [21] were strongly elevated in *Z. zerumbet* upon pathogen inoculation (Figs 1 & 2). *TP7*, a member of the peroxidase gene family was remained highly up-regulated in all the time periods examined in pathogen treated *Z. zerumbet* (Fig. 1; Table S1).

An ortholog of *COBRA LIKE 4* (*COBL4)* gene, which is expressed in vascular bundles in rice and positively regulate cell wall thickness and mechanical strength of cells, was strongly induced in pathogen-inoculated *Z. zerumbet* [38]. A member of the *DIRIGENT* gene family (*DIR22*), which modulate cell wall metabolism during stress adaptation and positively regulate cell-wall lignification upon pathogen infection [39] was also up-regulated in *Z. zerumbet* (Fig. 1; Table S1).

Biosynthesis and signalling of BR, GA and auxin

HMG-CoA reductase (HMGR) is a rate-limiting enzyme in the biosynthesis of mevalonate, the precursor of steroids, including BR [40]. The cytochrome P450 protein CYP90B1 encoded by *DWARF 4* (*DWF4*), which catalyze the C22-hydroxylation of campesterol is another important enzyme in the BR biosynthetic pathway [41]. Both *HMGR* and *DWF4* genes were down-regulated in *Z. zerumbet* in response to *P. myriotylum* (Fig. 3; Table S1). *SHAGGY-RELATED PROTEIN KINASE ETA/BRASSINOSTEROID INSENSITIVE 2* (*ASK7*/*BIN2*), a negative regulator of BR signaling [42] and an AP2/ERF transcription factor *RAV1*, a negative regulator of growth, which is suppressed during BR signaling [43], were up-regulated (Fig. 3; Table S1).

The *GIBBERELLIN 20 OXIDASE 1-D* (*GA20ox1D*), a key gene involved in gibberellic acid (GA) biosynthesis [44] and two members of the *GIBBERELLIN-3-BETA-DEOXYGENASE* gene family (*GA3OX1*, *GA3OX2*) that catalyze the

conversion of precursor GA3 into the bioactive form were down-regulated [45] (Fig. 3; Table S1). Also, a decline in the quantity of the transcripts was recorded for two GA regulated genes GA-Stimulated transcripts in *Arabidopsis* 6 (*GASA6*) [46] and *SQUAMOSA-PROMOTER-BINDING-PROTEIN-LIKE8* (*SPL8*) [47] in *Z. zerumbet* in response to *P. myriotylum* (Fig. 3; Table S1).

The expression of *INDOLE-3-ACETALDEHYDE OXIDASE1* (*AAO1*), which is involved in auxin biosynthesis [48] was suppressed in pathogen-inoculated *Z. zerumbet*. The *GH3-8* gene encoding an indole-3-acetic acid-amidosynthetase enzyme, which catalyzes the conjugation of auxin to amino acids and producing an inactive storage form of auxin [49], was strongly triggered (Fig. 3; Table S1). Two members of the *AUXIN RESPONSE FACTOR* transcription factors *ARF19-LIKE* and *ARF6* that activate auxin-responsive genes and two members of the auxin-responsive gene family *SMALL-AUXIN-UP RNA* (*SAUR 71*, *SAUR 32*), that also regulate cell expansion positively [50], were down-regulated in *Z. zerumbet* following *P. myriotylum* inoculation (Fig. 3; Table S1).

Penetration pattern of *P. myriotylum* in *Z. zerumbet*

Safranin-O staining of the transverse sections from collar region revealed the anatomy of the aerial stem in *Z. zerumbet* (Fig. 4a). The aerial-stem is composed of a central pith, which is adhered around by whorl leaf sheaths. Each leaf sheath consisted of closely packed mesophyll cells delimited by a layer of well-formed adaxial and a loosely formed abaxial epidermis. Each leaf sheath has one row of vascular bundles, whereas numerous vascular bundles are scatteredly arranged in the parenchymatous pith. The pith is delimited by an endodermis-like ring of thickly stained sclerenchyma cells (Fig. 4a).

389 The lactophenol-trypan blue staining of longitudinal sections of collar region
390 recognized an intracellular cell to cell penetration for *P. myriotylum* in *Z. zerumbet*
391 tissues (Fig. 4b, c). The pathogen hyphae were detected at the peripheral leaf sheath
392 whorl of the aerial-stem as early as 12 hpi (Fig. 4d). The hyphae were restricted at the
393 peripheral leaf sheath whorl and never extended into the pith region (Fig. 4d).

394 **Cell wall fortification pattern in *Z. zerumbet* following *P. myriotylum* ingress**

395 Phloroglucinol-HCl staining of the transverse section of collar region recognized the
396 lignification of the wall of mesophyll cells that surround vascular bundles in the leaf
397 sheath whorls at 12hpi (Fig. 5a). Staining intensity of the walls of these cells
398 increased progressively as the time elapsed after the pathogen inoculation. In addition,
399 the staining intensity of the wall of the mesophyll cells that occurred in between two
400 vascular bundles was also increased steadily (Fig. 5b). Finally, by 48hpi a ring of
401 lignified cells surrounding the vascular bundles and in some cases a barrage of
402 lignified mesophyll cells in between two vascular bundles were recognized in leaf
403 sheath whorls (Fig. 5c).

404 Correspondingly the total cell wall bound soluble lignin content of the collar
405 region steadily increased significantly ($p < 0.05$) from 12hpi to 48hpi (Fig. 6). The
406 DAB staining of the longitudinal section of the collar region detected an increase in
407 the staining intensity from 12hpi to 48hpi, indicating an increase in the accumulation
408 of H_2O_2 following *P. myriotylum* inoculation in *Z. zerumbet* (Fig. 7)
409

410 **Discussion**

411 Necrotrophs induce host *PME* and promote the demethylesterification of the cell wall
412 pectins, especially HG [11]. The demethylesterified HGs are more susceptible to

CDEs PG and PEL secreted by the pathogens, and also to host own PG and PEL [11,12]. The suppression of the host *PG* or *PEL* induces resistance against pathogens [13, 14]. The significant down-regulation of the *PME*, *PG*, *PEL* and *BURP12* in *Z. zerumbet* in response to *P. myriotylum* inoculation (Fig. 1; Table S1) may be a host mechanism to protect its cell wall from pathogen factors, which promote the cell wall loosening and the subsequent degradation [10–12, 14]. The up-regulation of the membrane-localized *PM H+ATPase* and the down-regulation of *FER* (Fig. 1; Table S1), which negatively regulate the *PM H+ATPase* [51] suggest the acidification of apoplast in *Z. zerumbet* in response to *P. myriotylum* to suppress pathogen colonization as reported in other plant species [33]. The *PME* is less active in acidic apoplast [51]. Pathogen needs an alkaline apoplast to promote infection and the pathogen effectors negatively regulate *PM H+ATPase* to alkalinize the extracellular region of the host [33]. In *Arabidopsis* that lack the FER activity, this alkalinization effect is low and so also is the rate of infection [52]. Together, the data indicate a coordinated reprogramming of transcriptional machinery in *Z. zerumbet* against *P. myriotylum* infection to minimize the cell wall damage by suppressing the expression of host genes, which encode the molecules that are known to be the target of pathogen factors.

The changes triggered by pathogen in the pectin composition of host cell wall results in the production of OGs [11, 12]. The OGs act as a DAMP [10] and the WAKs bind with OGs and activate host immunity [18]. In wild strawberry, an optimum pool of OGs produced by the degradation of partial demethylesterified HG is needed to elicit the resistance reactions against the necrotrophic pathogen *Botrytis cinerea* [12]. The up-regulation of the gene encoding the PG enzyme QRT3 [32] suggest changes in pectin composition in *Z. zerumbet* in response to *P. myriotylum*.

438 Changes in cell wall pectin trigger the *WAK2* expression and it leads to the induction
439 of stress related genes [18]. The significant up-regulation of *WAK2-Like* genes and
440 *QRT3* noted in the present study (Fig. 1; Table S1) indicate a possible involvement of
441 OGs and *WAK* mediated signaling in the resistance response of *Z. zerumbet* to *P.*
442 *myriotylum*.

443 The primary cell wall of a cell undergoes enzymatic loosening in order to
444 increase its extensibility during the process of elongation [16]. The transcriptional
445 data indicates the suppression of the cell wall loosening and elongation process in *Z.*
446 *zerumbet* at multiple levels following *P. myriotylum* inoculation. The genes encoding
447 the two key enzymes XTH and PME that involved in cell wall loosening [16] were
448 down regulated in *Z. zerumbet* following *P. myriotylum* inoculation. In addition, the
449 expression of *FER*, *HERK1* and *ER*, the three membrane-localized receptor like
450 kinases with a crucial role in cell expansion [34, 35] were suppressed in *Z. zerumbet*
451 (Fig. 1; Table S1). Homozygous *fer* mutations are reported to impart resistance to
452 powdery mildew infection in *Arabidopsis* [53]. Similarly, the biosynthesis and
453 signaling of the phytohormones BR, GA and auxin that are involved in the regulation
454 of cell elongation were also suppressed in *Z. zerumbet* following pathogen inoculation
455 (Fig. 3; Table S1). Increase in the concentration of auxin and the activity of XTH
456 together with cell wall loosening and cell elongation precede club root infection
457 caused by *Plasmodiophora brassicae* in Chinese cabbage [15]. *P. graminicola* is
458 known to hijacks the brassinosteroid (BR) signaling machinery in rice and exploits
459 BRs as virulence factors to inflict disease [6]. Overall the data suggest that the
460 suppression of cell wall loosening and cell elongation is an important component of
461 host defense in *Z. zerumbet* against *P. myriotylum* infection. This is possibly to

preempt pathogen effort to penetrate host cells as the pathogens prefer to enter the cell through the loosened and elongating portion of the cell wall [15, 17].

Constitutive expression of cell wall invertase, which irreversibly catalyzes the cleavage of sucrose into fructose and glucose, enhances resistance to *Magnaporthe oryzae* in rice [36]. In *Vitis vinifera*, the effectors secreted by *Botrytis cinerea* trigger the sugar transporter *SWEET* gene to acquire sugar necessary for its growth [37]. In *Arabidopsis*, the *SWEET* gene knockout mutants are less susceptible to *B. cinerea* [37]. The strong induction of *INV3* and the down-regulation of *SWEET* gene recorded in the present study (Fig. 1; Table S1) suggest the accumulation of sugar in *Z. zerumbet* following pathogen inoculation and prevention of pathogen access to this sugar pool. Taken together the data suggest a role for sugar signaling in mediating host resistance in *Z. zerumbet* as the accumulation of hexoses induces the constitute expression of defense-related genes, H_2O_2 accumulation and the thickening of cell wall at the site of infection [36].

The expression of *CESA4*/*IRX5* and *WAT1* that are involved in the deposition of cellulose in secondary cell wall was down-regulated in *Z. zerumbet* following *P. myriotylum* inoculation (Fig. 1; Table S1). The suppression of *CESA4*/*IRX5* and *WAT1* contributes resistance to necrotrophic pathogens in *Arabidopsis* [23, 24]. Suppression of genes involved in the deposition of cellulose in the secondary cell wall or the cell expansion is known to trigger host defense and the lignification cell walls [25]. In parallel with the previous reports [25, 54], the genes such as *PAL*, *4CL2*, *CCR*, *COMT1*and *CAD2* that are involved in the monolignol biosynthesis in the phenylpropanoid biosynthetic pathway were strongly up-regulated in *Z. zerumbet* following *P. myriotylum* inoculation (Figs 1 & 2; Table S1). In addition, two key genes *COBL4* and *DIR22*, which positively regulate lignification and mechanical

strength of cells upon pathogen infection [38, 39], were also strongly up-regulated (Fig. 1; Table S1). The monolignols are synthesized in the cytoplasm and are transported to apoplast. In the apoplast the monolignols are polymerized to lignin in the presence of peroxidase enzymes and H_2O_2 [21]. Strong up-regulation of one of the peroxidase enzyme genes *TP7* (Fig. 1; Table S1) and the accumulation of H_2O_2 around vascular bundles in leaf sheaths (Fig. 7) shows the increased lignin deposition in the cells surrounding vascular bundles in leaf sheaths as the pathogen penetration progresses in *Z. zerumbet*.

Corroborating the up-regulation of genes involved in monolignol biosynthesis and lignin polymerization, the phloroglucinol-HCl staining of the collar sections clearly showed the formation of a layer of lignified mesophyll cells surrounding vascular bundles and a patch of lignified cells in between vascular bundles in leaf sheaths (Fig. 5). Further, the total lignin content significantly increased in pathogen inoculated *Z. zerumbet* (Fig. 6). The lactophenol-trypan blue staining of collar sections showed that the hyphal growth is restricted at the leaf sheaths and is not extended into the pith (Fig. 4d). Thus, the histochemical data clearly showed the early and robust induction of lignin synthesis in *Z. zerumbet* following *P. myriotylum* infection and the formation of a barrier of lignified mesophyll cells to prevent the entry of pathogen into the vascular bundles in the leaf sheaths and into the pith region through which principal portion of the connective tissues passes in the aerial stem. The *Pythium* is a vascular wilt pathogen and vascular bundles of the host are the targets for its colonization. Wilting occurs only when pathogen enters the vascular tissues of the host [55]. The lignification and the cell wall strengthening constitute an important strategy employed by the host to suppress necrotrophic infection [20]. The study illustrates a key role for cell wall fortification in imparting resistance against *P.*

myriotylum in *Z. zerumbet* by preventing the colonization of the pathogen in the vascular tissues and ensuring the transport system of the plants remain unaffected by the pathogen invasion.

To conclude, the study provides a strong evidence for a crucial role for cell wall signaling in mediating *P. myriotylum* resistance in *Z. zerumbet*. Results highlight the negative regulation of cell wall loosening and cell elongation processes in the post inoculated host to suppress the pathogen penetration. Alongside, the cell walls were reinforced by lignin deposition to doubly ensure the protection from pathogen infection.

ANOWKLEDGEMENTS

KAG and LA thank Council for Scientific and Industrial Research (CSIR), Government of India and Kerala State Council for Science technology and Environment (KSCSTE), Government of Kerala for research fellowship, respectively. GT acknowledge Council for Scientific and Industrial Research (CSIR), Government of India for research grant (Sanction Number 38 (1397)/14/EMR-II Dated 30/10/2014). We would like to thank Genotypic Technology PVT. LTD, Bengaluru, India and University of Delhi South Campus Microarray Centre (UDSCMAC), University of Delhi, India for RNA-Seq and microarray analyses respectively.

542 **Reference**

543

544 [1] D.P. Le, M. Smith, G.W. Hudler, E. Aitken, Pythium soft rot of ginger:
545 Detection and identification of the causal pathogens, and their control, Crop
546 Prot. 65 (2014) 153–167. doi:10.1016/j.cropro.2014.07.021.
547 [2] P.A. Okubara, M.B. Dickman, A.E. Blechl, Molecular and genetic aspects of
548 controlling the soilborne necrotrophic pathogens *Rhizoctonia* and *Pythium*,
549 Plant Sci. 228 (2014) 61–70. doi:10.1016/j.plantsci.2014.02.001.
550 [3] P.G. Kavitha, G. Thomas, Population genetic structure of the clonal plant
551 *Zingiber zerumbet* (L.) Smith (Zingiberaceae), a wild relative of cultivated
552 ginger, and its response to *Pythium aphanidermatum*, Euphytica. 160 (2008)
553 89–100. doi:10.1007/s10681-007-9557-5.
554 [4] P. Vijayan, J. Shockey, C.A. Levesque, R.J. Cook, J. Browse, A role for
555 jasmonate in pathogen defense of *Arabidopsis*, Proc. Natl. Acad. Sci. 95 (1998)
556 7209–7214. doi:10.1073/pnas.95.12.7209.
557 [5] B.A.T. Adie, J. Perez-Perez, M.M. Perez-Perez, M. Godoy, J.-J. Sanchez-
558 Serrano, E.A. Schmelz, R. Solano, ABA is an essential signal for plant
559 resistance to pathogens affecting JA biosynthesis and the activation of defenses
560 in *Arabidopsis*, Plant Cell. 19 (2007) 1665–1681. doi:10.1105/tpc.106.048041.
561 [6] D. De Vleesschauwer, E. Van Buyten, K. Satoh, J. Balidion, R. Mauleon, I.-R.
562 Choi, C. Vera-Cruz, S. Kikuchi, M. Hofte, Brassinosteroids antagonize
563 gibberellin- and salicylate-mediated root immunity in rice, Plant Physiol. 158
564 (2012) 1833–1846. doi:10.1104/pp.112.193672.
565 [7] S.K. Chand, S. Nanda, E. Rout, J.N. Mohanty, R. Mishra, R.K. Joshi, *De novo*
566 sequencing and characterization of defense transcriptome responsive to
567 *Pythium aphanidermatum* infection in *Curcuma longa* L., Physiol. Mol. Plant
568 Pathol. 94 (2016) 27–37. doi:10.1016/j.pmpp.2016.03.008.
569 [8] P.G. Kavitha, G. Thomas, Defence transcriptome profiling of *Zingiber*
570 *zerumbet* (L.) Smith by mRNA differential display, J. Biosci. 33 (2008) 81–90.
571 doi:10.1007/s12038-008-0002-2.
572 [9] P.G. Kavitha, G. Thomas, Expression analysis of defense-related genes in
573 *Zingiber* (Zingiberaceae) species with different levels of compatibility to the
574 soft rot pathogen Pythium aphanidermatum, Plant Cell Rep. 27 (2008) 1767–
575 1776. doi:10.1007/s00299-008-0594-x.

[10] M. Nafisi, L. Fimognari, Y. Sakuragi, Interplays between the cell wall and phytohormones in interaction between plants and necrotrophic pathogens, Phytochemistry. 112 (2015) 63–71. doi:10.1016/j.phytochem.2014.11.008.

[11] A. Raiola, V. Lionetti, I. Elmaghraby, P. Immerzeel, E.J. Mellerowicz, G. Salvi, F. Cervone, D. Bellincampi, Pectin Methylesterase is induced in *Arabidopsis* upon infection and is necessary for a successful colonization by necrotrophic pathogens, Mol. Plant-Microbe Interact. Mol. Plant-Microbe Interact. 24 (2011) 432–440. doi:10.1094.

[12] S. Osorio, C. Castillejo, M.A. Quesada, N. Medina-Escobar, G.J. Brownsey, R. Suau, A. Heredia, M.A. Botella, V. Valpuesta, Partial demethylation of oligogalacturonides by pectin methyl esterase 1 is required for eliciting defence responses in wild strawberry (*Fragaria vesca*), Plant J. 54 (2008) 43–55. doi:10.1111/j.1365-313X.2007.03398.x.

[13] J.P. Vogel, T.K. Raab, C. Schiff, S.C. Somerville, *PMR6* , a pectate lyase-like gene required for powdery mildew susceptibility in *Arabidopsis*, Plant Cell 14 (2002) 2095–2106. doi:10.1105/tpc.003509.sis.

[14] D. Cantu, A.R. Vicente, L.C. Greve, F.M. Dewey, A.B. Bennett, J.M. Labavitch, A.L.T. Powell, The intersection between cell wall disassembly, ripening, and fruit susceptibility to *Botrytis cinerea*, Proc. Natl. Acad. Sci. U. S. A. 105 (2008) 859–864. doi:10.1073/pnas.0709813105.

[15] S. Devos, K. Vissenberg, J.-P. Verbelen, E. Prinsen, Infection of Chinese cabbage by *Plasmodiophora* of Chinese infection growth : impacts of plant leads to a stimulation brassicae and hormone balance on cell wall metabolism, New Phytol. 166 (2005) 241–250. doi:10.1111/j.1469-8137.2004.01304.x/full.

[16] Y. Chebli, A. Geitmann, Cellular growth in plants requires regulation of cell wall biochemistry, Curr. Opin. Cell Biol. 44 (2017) 28–35. doi:10.1016/j.ceb.2017.01.002.

[17] U. Gunawardena, M.C. Hawes, Tissue specific localization of root infection by fungal pathogens: role of root border cells., Mol. Plant-Microbe Interact. 15 (2002) 1128–1136. doi:10.1094/MPMI.2002.15.11.1128.

[18] B.D. Kohorn, S.L. Kohorn, T. Todorova, G. Baptiste, K. Stansky, M. McCullough, A dominant allele of *Arabidopsis* pectin-binding wall-associated kinase induces a stress response suppressed by MPK6 but not MPK3 mutations, Mol. Plant. 5 (2012) 841–851. doi:10.1093/mp/ssr096.

[19] L. De Bruyne, M. Höfte, D. De Vleesschauwer, Connecting growth and defense: The emerging roles of brassinosteroids and gibberellins in plant innate immunity, Mol. Plant. 7 (2014) 943–959. doi:10.1093/mp/ssu050.

[20] L. Xu, L. Zhu, L. Tu, L. Liu, D. Yuan, L. Jin, L. Long, X. Zhang, Lignin metabolism has a central role in the resistance of cotton to the wilt fungus *Verticillium dahliae* as revealed by RNA-Seq-dependent transcriptional analysis and histochemistry, J. Exp. Bot. 62 (2011) 5607–5621. doi:10.1093/jxb/err245.

[21] C.M. Fraser, C. Chapple, The phenylpropanoid pathway in *Arabidopsis*, Arab. B. 9 (2011) e0152. doi:10.1199/tab.0152.

[22] B. Asselbergh, K. Curvers, S.C. Franca, K. Audenaert, M. Vuylsteke, F. Van Breusegem, M. Hofte, Resistance to *Botrytis cinerea* in sitiens, an abscisic acid-deficient tomato mutant, involves timely production of hydrogen peroxide and cell wall modifications in the epidermis, Plant Physiol. 144 (2007) 1863–1877. doi:10.1104/pp.107.099226.

[23] C. Hernandez-Blanco, D.X. Feng, J. Hu, A. Sanchez-Vallet, L. Deslandes, F. Llorente, M. Berrocal-Lobo, H. Keller, X. Barlet, C. Sanchez-Rodriguez, L.K. Anderson, S. Somerville, Y. Marco, A. Molina, Impairment of cellulose synthases required for *Arabidopsis* secondary cell wall formation enhances disease resistance, Plant Cell. 19 (2007) 890–903. doi:10.1105/tpc.106.048058.

[24] N. Denancé, P. Ranocha, N. Oria, X. Barlet, M.P. Rivière, K.A. Yadeta, L. Hoffmann, F. Perreau, G. Clément, A. Maia-Grondard, G.C.M. Van Den Berg, B. Savelli, S. Fournier, Y. Aubert, S. Pelletier, B.P.H.J. Thomma, A. Molina, L. Jouanin, Y. Marco, D. Goffner, *Arabidopsis wat1* (*walls are thin1*)-mediated resistance to the bacterial vascular pathogen, *Ralstonia solanacearum*, is accompanied by cross-regulation of salicylic acid and tryptophan metabolism, Plant J. 73 (2013) 225–239. doi:10.1111/tpj.12027.

[25] A. Cano-delgado, S. Penfield, C. Smith, M. Catley, M.B. Ã, Reduced cellulose synthesis invokes lignincation and defense responses in *Arabidopsis thaliana*, Plant J. 34 (2003) 351–362. doi:10.1046/j.1365-313X.2003.01729.x.

[26] C.I.N. Unamba, A. Nag, R.K. Sharma, Next generation sequencing technologies: The doorway to the unexplored genomics of non-model plants, Front. Plant Sci. 6 (2015). doi:10.3389/fpls.2015.01074.

[27] A. Kumar, S. T. Reeja, R. Suseela Bhai, K. N. Shiva, Distribution of *Pythium*

644 *myriotylum* Drechsler causing soft rot of ginger, J. Spices Aromat. Crops. 17
645 (2008) 5–10.
646 [28] C. A. Levesque, A. W. De Cock, Molecular phylogeny and taxonomy of the
647 genus *Pythium*. Mycol. Res. 108 (2004) 1363-1383.
648 doi:10.1017/S0953756204001431
649 [29] R.A. Salzman, T. Fujita, K. Zhu-Salzman, P. Hasegawa, R. Bressan, An
650 improved RNA isolation method for plant tissues containing high levels of
651 phenolic compounds or carbohydrates, Plant Mol. Biol. Rep. 17 (1999) 11-17
652 .doi:10.1023/A:1007520314478.
653 [30] K. Iiyama, A.F.A. Wallis, Determination of lignin in herbaceous plants by an
654 improved acetyl bromide procedure, J. Sci. Food Agric. 51 (1990) 145–161.
655 doi:10.1002/jsfa.2740510202.
656 [31] X. Ding, X. Hou, K. Xie, L. Xiong, Genome-wide identification of BURP
657 domain-containing genes in rice reveals a gene family with diverse structures
658 and responses to abiotic stresses, Planta. 230 (2009) 149–163.
659 doi:10.1007/s00425-009-0929-z.
660 [32] S.Y. Rhee, E. Osborne, P.D. Poindexter, C.R. Somerville, Microspore
661 Separation in the *quartet 3* mutants of *Arabidopsis* is impaired by a defect in a
662 developmentally regulated polygalacturonase is required for pollen mother cell
663 wall degradation, Plant Physiol. 133 (2003) 1170–1180.
664 doi/10.1104/pp.103.028266..
665 [33] J.M. Elmore, G. Coaker, The role of the plasma membrane H+-ATPase in
666 plant-microbe interactions, Mol. Plant. 4 (2011) 416–427.
667 doi:10.1093/mp/ssq083.
668 [34] H. Guo, L. Li, H. Ye, X. Yu, A. Algreen, Y. Yin, Three related receptor-like
669 kinases are required for optimal cell elongation in *Arabidopsis thaliana*, Proc.
670 Natl. Acad. Sci. U. S. A. 106 (2009) 7648-7653.
671 doi:10.1073/pnas.0812346106.
672 [35] E.D. Shpak, Diverse roles of *ERECTA* family genes in plant development, J.
673 Integr. Plant Biol. 55 (2013) 1238–1250. doi:10.1111/jipb.12108.
674 [36] L. Sun, D. lei Yang, Y. Kong, Y. Chen, X.Z. Li, L.J. Zeng, Q. Li, E.T. Wang,
675 Z.H. He, Sugar homeostasis mediated by cell wall invertase GRAIN
676 INCOMPLETE FILLING 1 (GIF1) plays a role in pre-existing and induced
677 defence in rice, Mol. Plant Pathol. 15 (2014) 161–173.

678 doi:10.1111/mpp.12078.
679 [37] J. Chong, M.C. Piron, S. Meyer, D. Merdinoglu, C. Bertsch, P. Mestre, The
680 SWEET family of sugar transporters in grapevine: VvSWEET4 is involved in
681 the interaction with *Botrytis cinerea*, J. Exp. Bot. 65 (2014) 6589–6601.
682 doi:10.1093/jxb/eru375.
683 [38] F. Roudier, The COBRA Family of putative GPI-anchored proteins in
684 *Arabidopsis*. A new fellowship in expansion, Plant Physiol. 130 (2002) 538–
685 548. doi:10.1104/pp.007468.
686 [39] C. Paniagua, A. Bilkova, P. Jackson, S. Dabravolski, W. Riber, V. Didi, J.
687 Houser, N. Gigli-Bisceglia, M. Wimmerova, E. Budínská, T. Hamann, J.
688 Hejatko, Dirigent proteins in plants: modulating cell wall metabolism during
689 abiotic and biotic stress exposure, J. Exp. Bot. 68 (2017) 3287–3301.
690 doi:10.1093/jxb/erx141.
691 [40] K. Ohyama, M. Suzuki, K. Masuda, S. Yoshida, T. Muranaka, Chemical
692 phenotypes of the *hmg1* and *hmg2* mutants of *Arabidopsis* demonstrate the *in-*
693 *planta* role of HMG-CoA reductase in triterpene biosynthesis, Chem Pharm
694 Bull. 55 (2007) 1518–1521. doi:10.1248/cpb.55.1518.
695 [41] S. Fujita, T. Ohnishi, B. Watanabe, T. Yokota, S. Takatsuto, S. Fujioka, S.
696 Yoshida, K. Sakata, M. Mizutani, *Arabidopsis* CYP90B1 catalyses the early C-
697 22 hydroxylation of C27, C28 and C29 sterols, Plant J. 45 (2006) 765–774.
698 doi:10.1111/j.1365-313X.2005.02639.x.
699 [42] J. Li, K.H. Nam, Regulation of brassinosteroid signaling by a GSK3 /
700 SHAGGY-Like Kinase, Science. 295 (2002) 1299–1301.
701 doi:10.1126/science.1065769.
702 [43] Y.X. Hu, Y.H. Wang, X.F. Liu, J.Y. Li, *Arabidopsis* RAV1 is down-regulated
703 by brassinosteroid and may act as a negative regulator during plant
704 development, Cell Res. 14 (2004) 8–15. doi:10.1038/sj.cr.7290197.
705 [44] N.E.J. Appleford, D.J. Evans, J.R. Lenton, P. Gaskin, S.J. Croker, K.M. Devos,
706 A.L. Phillips, P. Hedden, Function and transcript analysis of gibberellin-
707 biosynthetic enzymes in wheat, Planta. 223 (2006) 568–582.
708 doi:10.1007/s00425-005-0104-0.
709 [45] M.G. Mitchum, S. Yamaguchi, A. Hanada, A. Kuwahara, Y. Yoshioka, T.
710 Kato, S. Tabata, Y. Kamiya, T.P. Sun, Distinct and overlapping roles of two
711 gibberellin 3-oxidases in *Arabidopsis* development, Plant J. 45 (2006) 804–

818. doi:10.1111/j.1365-313X.2005.02642.x.

[46] J. Qu, S.G. Kang, C. Hah, J.C. Jang, Molecular and cellular characterization of GA-stimulated transcripts GASA4 and GASA6 in *Arabidopsis thaliana*, Plant Sci. 246 (2016) 1–10. doi:10.1016/j.plantsci.2016.01.009.

[47] Y. Zhang, S. Schwarz, H. Saedler, P. Huijser, SPL8, a local regulator in a subset of gibberellin-mediated developmental processes in *Arabidopsis*, Plant Mol. Biol. 63 (2007) 429–439. doi:10.1007/s11103-006-9099-6.

[48] M. Seo, S. Akaba, T. Oritani, M. Delarue, C. Bellini, M. Caboche, T. Koshiba, Higher activity of an aldehyde oxidase in the auxin-overproducing *superroot1* mutant of *Arabidopsis thaliana*, Plant Physiol. 116 (1998) 687–693. doi:10.1104/pp.116.2.687.

[49] X. Ding, Y. Cao, L. Huang, J. Zhao, C. Xu, X. Li, S. Wang, Activation of the indole-3-acetic acid-amido synthetase GH3-8 suppresses expansin expression and promotes salicylate- and jasmonate-independent basal immunity in rice, Plant Cell. 20 (2008) 228–240. doi:10.1105/tpc.107.055657.

[50] K.I. Hayashi, The interaction and integration of auxin signaling components, Plant Cell Physiol. 53 (2012) 965–975. doi:10.1093/pcp/pcs035.

[51] L. Hocq, J. Pelloux, V. Lefebvre, Connecting pectin remodeling to acid growth, Trends Plant Sci. 22 (2017) 20–29. doi:10.1016/j.tplants.2016.10.009.

[52] S. Masachis, D. Segorbe, D. Turrà, M. Leon-Ruiz, U. Fürst, M. El Ghalid, G. Leonard, M.S. López-Berges, T.A. Richards, G. Felix, A. Di Pietro, A fungal pathogen secretes plant alkalinizing peptides to increase infection, Nat. Microbiol. 1 (2016) 1–8. doi:10.1038/nmicrobiol.2016.43.

[53] S.A. Kessler, H. Shimosato-Asano, N.F. Keinath, S.E. Wuest, G. Ingram, R. Panstruga, U. Grossniklaus, Conserved molecular components for pollen tube reception and fungal invasion, Science. 330 (2010) 968–971. doi:10.1126/science.1195211.

[54] L. Denness, J.F. McKenna, C. Segonzac, A. Wormit, P. Madhou, M. Bennett, J. Mansfield, C. Zipfel, T. Hamann, Cell wall damage-induced lignin biosynthesis is regulated by a reactive oxygen species- and jasmonic acid-dependent process in *Arabidopsis*, Plant Physiol. 156 (2011) 1364–1374. doi:10.1104/pp.111.175737.

[55] K.A. Yadeta, B.P.H. J. Thomma, The xylem as battleground for plant hosts and vascular wilt pathogens, Front. Plant Sci. 4:97 (2013) 1–12.

746 doi:10.3389/fpls.2013.00097.

747

748

749

750

751

752

753

754

755

756

757

758

759

760

761

762

763

764

765

766

767

768

769

770

771

772

773

774

775

776

777

Suppoting Information legend

Supplementary Table 1. Genes that are signficantly differentially expressed in *Z. zerumebt* following *Pythium* inoculation and used in the study together with their expression profile based on digital gene expression (DGE) computed from transcriptome analysis and gene expression microarray or RT-qPCR. Values in bold indicate significant ($p < 0.05$) modulatioin obtained for a probe in gene expression microarray analysis

Figure Legends

Figure 1. Heat map showing the relative fold change in the transcript levels of 27 genes with cell wall related functions in *Z. zerumbet* at 18hpi, 36hpi and 48hpi with *P. myriotylum*. Fold changes were determined by the gene expression microarray analysis of RNA samples isolated from the untreated control plants and the treated plants at the respective time periods post inoculation with *P. myriotylum*. The probe sequences are given in Table S1. The gene abbreviations are as in the text and the Table S1.

Figure 2. Histograms showing the relative fold change in the transcript levels of the genes *PAL* (a), *CCR* (b), *COMT1* (c) and *CAD2* (d) in *Z. zerumbet* at 12hpi, 24hpi, 36hpi, 48hpi and 60hpi with *P. myriotylum*. Fold changes were determined by RT-qPCR analysis of the RNA samples isolated from the untreated control plants and the treated plants at the respective time periods post inoculation with *P. myriotylum*. Asterisks indicate significant difference ($p < 0.05$) in relation to control (0hpi). The gene abbreviations are as in the text and Table S1.

Figure 3. Heat map showing the relative fold change in the transcript levels of 15 genes involved in the biosynthesis and signaling of BR, GA and auxin in *Z. zerumbet* at 18hpi, 36hpi and 48hpi with *P. myriotylum*. Fold changes were determined by the

gene expression microarray analysis of RNA samples isolated from the untreated control plants and the treated plants at the respective time periods post inoculation with *P. myriotylum*. The probe sequences are given in Table S1. The gene abbreviations are as in the text and the Table S1.

Figure 4. The basic anatomy of *Z. zerumbet* aerial-stem and the penetration pattern of *P. myriotylum* in the host tissue. Safranin-O staining of transverse section of collar region revealed that the aerial-stem is composed of central pith and whorls of strongly adhered leaf sheaths (a). Lactophenol-trypan blue stained longitudinal section of the collar region of un-inoculated control plant (b). The lactophenol-trypan blue staining of longitudinal sections of collar region recognized that the *P. myriotylum* has an intra-cellular penetration pattern in *Z. zerumbet* (c) and the pathogen spread is limited to the peripheral leaf sheath whorls (d). ADE-adaxial epidermis; ABE-abaxial epidermis; PLS-peripheral leaf sheath; VB-vascular bundle; ELR-endodermis like ring; PT-pith; Pm-*P. myriotylum* hyphae.

Figure 5. Phloroglucinol-HCl stained transverse section of the collar region showing the pattern of lignin deposition in *Z. zerumbet* following *P. myriotylum* inoculation. No lignin deposition was found in the mesophyll cells surrounding the vascular bundles in the leaf sheath in the untreated control plant (a). Lignin deposition in the mesophyll cells surrounding the vascular bundles in the leaf sheath increased following *P. myriotylum* inoculation (b: 12hpi) and in certain cases a bridge of lignified mesophyll cells were formed between vascular bundles (c: 48hpi). Arrow indicates lignified mesophyll cells. VB-vascular bundle

Figure 6. The cell wall bound total lignin content of the collar region of the aerial-stem of Z. *zerumbet* in untreated control plants (0 hrs) and at 12hpi, 24hpi, 36hpi and 48hpi with *P. myriotylum*.

828 **Figure 7**. DAB-stained longitudinal section of collar region of the aerial-stem of *Z.*
829 *zerumbet* in the untreated control plant (a) and in the treated plant at 24hpi with *P.*
830 *myriotylum* (b). VB-vascular bundle.

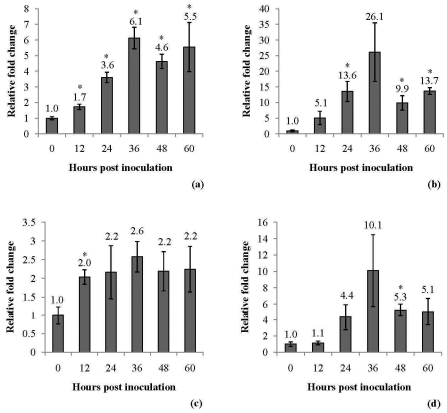

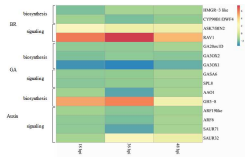

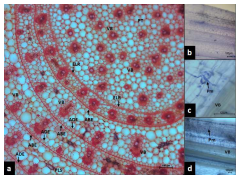

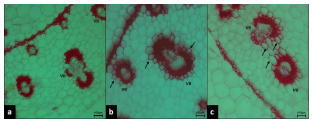

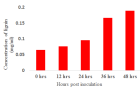

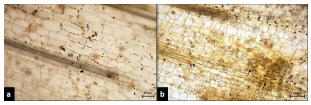

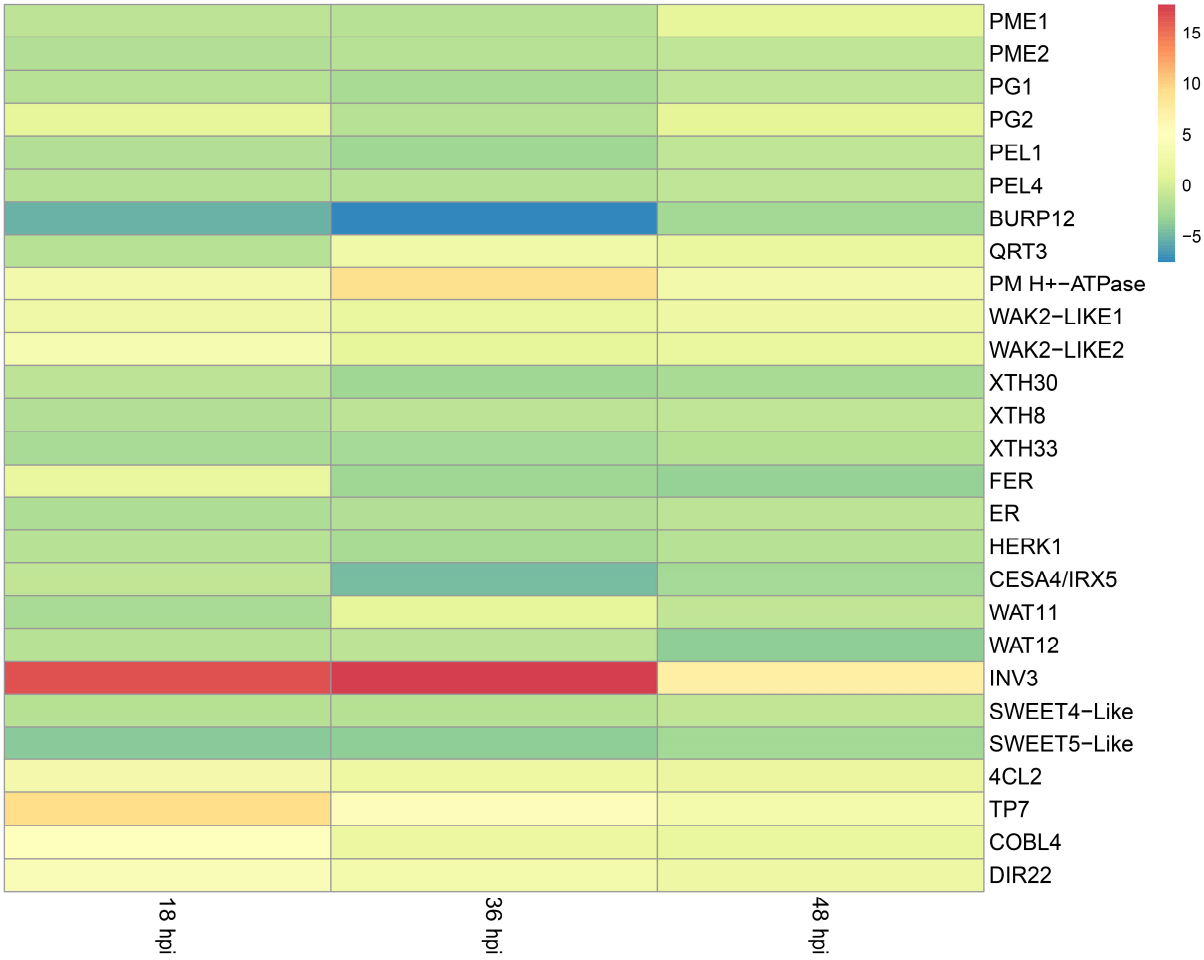

- Transcriptional changes of cell-wall related genes and histopathology were examined in resistant *Zingiber zerumbet* against *Pythium myriotylum* infection
- Many genes that promote cell wall loosening and cell elongation were suppressed.
- Several monolignol biosynthetic pathway genes were up-regulated.
- Histochemistry revealed H_2O_2 accumulation, increased lignification of the mesophyll cells in the leaf sheath and the significant increase in total lignin content.
- Pathogen hyphae were restricted to peripheral leaf sheath and were not extended into the pith
- The study illustrates a coordinated transcriptional reprogramming of cell wall-associated genes, and a key role for cell wall fortification in preventing pathogen colonization in the vascular tissues.